VOLCANO DEFORMATION AND MODELING ON ACTIVE VOLCANOES IN THE PHILIPPINES FROM ALOS INSAR TIME SERIES

Anieri M. Morales Rivera [(1)], Falk Amelung [(1)], Rodrigo Eco [(2)]

[(1)] University of Miami, Department of Marine Geosciences, 4600 Rickenbacker Cswy, Miami, FL, 33136, USA, Emails: amorales@rsmas.miami.edu, famelung@rsmas.miami.edu

[(2)] National Institute of Geological Sciences, University of the Philippines, C. P. Garcia Ave. corner Velasquez St., University of the Philippines, Diliman, Quezon City, 1101, Philippines, Email: narod.eco@gmail.com

ABSTRACT

Bulusan, Kanlaon, and Mayon volcanoes have erupted over the last decade, and Taal caldera showed signs of volcanic unrest within the same time range. Eruptions at these volcanoes are a threat to human life and infrastructure, having over 1,000,000 people living within 10 km from just these 4 volcanic centers. For this reason, volcano monitoring in the Philippines is of extreme importance.

We use the ALOS-1 satellite from the Japanese Aerospace Exploration Agency (JAXA) to make an InSAR time series analysis over Bulusan, Kanlaon, Mayon, and Taal volcanoes for the 2007-2011 period. Time-dependent deformation was detected at all of the volcanoes. Deformation related to changes in pressurization of the volcanic systems was found on Taal caldera and Bulusan volcanoes, with best fitting Mogi sources located at half-space depths of 3.07 km and 0.5 km respectively.

1. INTRODUCTION

Among the many benefits of satellite based remote sensing is providing global coverage for various volcano monitoring techniques. Satellite-based Interferometric Synthetic Aperture Radar (InSAR) is an example of a successful monitoring method that has provided the opportunity to detect and measure volcanic deformation months to years prior to volcanic eruptions [1]. The deformation signals detected by InSAR on volcanoes can be related to changes in pressurization of the volcanic systems, and are occasionally the earliest indicators of volcanic unrest [2], proving its potential for early warning systems.

According to the Philippine Institute of Volcanology and Seismology (PHIVOLCS), there are 23 active volcanoes in the Philippines. PHIVOLCS reported eruptions at Mayon, Bulusan, and Kanlaon volcanoes, and signs of volcanic unrest at Taal Caldera over the last decade (Tab. 1). Eruptions at these volcanoes are a threat to human life and infrastructure, having over 1,000,000 people living within 10 km from just these 4 volcanic centers (Smithsonian Institute, Global volcanism report, available at http://www.volcano.si.edu). For this reason, monitoring volcanic unrest in this area is of extreme importance.

Table 1. Volcanic eruptions in the Philippines during 2007-2011 (Smithsonian Institute, Global volcanism report, available at http://www.volcano.si.edu)

Volcano	Eruption Start	Eruption End
Mayon	08/10/2008	08/10/2008
	09/15/2009	01/01/2010
Bulusan	10/10/2006	10/04/2007
	11/06/2010	05/13/2011

We use the ALOS-1 satellite from the Japanese Aerospace Exploration Agency (JAXA), which acquired a global L-band data set of nearly 20 acquisitions during 2007-2011, to make an InSAR time series analysis over Mayon, Bulusan, Kanlaon, and Taal volcanoes (Fig. 1). The purpose is to determine if volcanic deformation can be detected with this data, and to present kinematic models that constrain the magmatic source characteristics for the cases were deformation is related to changes in pressurization of the system.

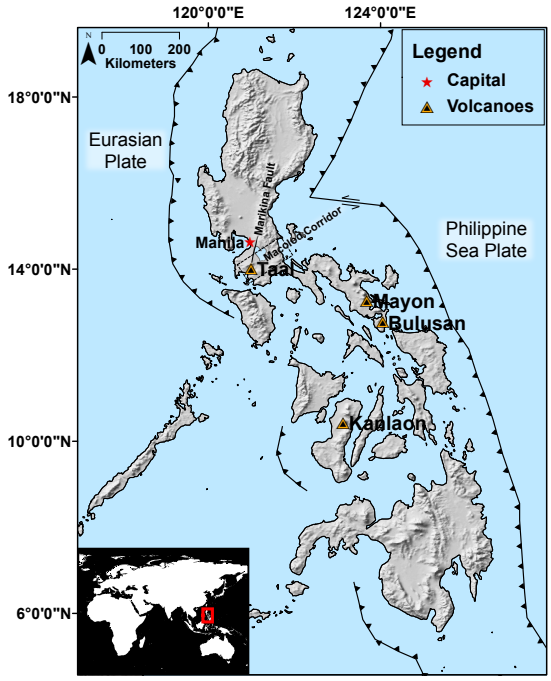

Figure 1. Targeted volcanoes in the Philippines

2. METHODS

2.1. InSAR data processing

The interferograms used in this study were processed using the Gamma SAR and Interferometric Processing Software [3] to focus the raw SAR images and generate the single looking complex images that were then used to generate the interferograms with the ROI_PAC SAR Software [4]. The interferograms were phase unwrapped using the SNAPHU algorithm [5]. Interferograms with perpendicular baselines of less than 1,500 meters were selected using the Delaunay method. We successively add all interferograms with perpendicular baselines less than 400 meters, temporal baselines of less than 2 years, and temporal baselines with more than two years apart but within two months of each other. Exceptions were made to these selection parameters in cases where the temporal coherence was generally high (higher than 0.7). Unwrapping error corrections were made to interferograms using a phase closure technique based on the triangular consistency of interferograms, developed at the University of Miami (Heresh Fattahi, personal communication).

2.2. InSAR time series generation

The time-series were generated with the PySAR software developed at the University of Miami (Heresh Fattahi, personal communication) by using the SBAS method [6] and making further corrections. The time-series were corrected for DEM errors after the inversion of the interferograms to remove the dependence between the perpendicular baseline and displacement history [7]. Time series were also corrected for phase ramp errors by estimating the linear surface that fits the interferometric phase [8]. Velocity maps were constructed from the corrected time-series to visualize the average displacement rates over the study area.

2.3. Ionospheric and atmospheric errors

Ionospheric noise corrections were not made but we can identify the dates that are partly affected by ionosphere by identifying outliers in the time series plot and analysing individual interferograms. Interferograms affected by ionosphere show distinct striking and decorrelation features, so the evident dates that are moderately or severely affected by ionospheric noise are eliminated prior to the inversion of interferograms. The dates were eliminated in order to obtain velocity maps that display a more accurate average displacement rate.

The following methods were used to identify and reduce atmospheric noise near the volcanoes. Time series plots were made for volcanoes with points of similar elevation to identify if the line of sight (LOS) displacement patterns and magnitudes are similar, which would suggest phase delay errors due to the layered atmosphere [9]. If similar patterns exist with different magnitudes, it could suggest the presence of localized atmospheric delay errors or a real deformation signal. For this case, we change the reference pixel to a point as close as possible or on the volcano of interest (within less than 10 km from the deformation signal). This is done under the assumption that no deformation is present on the reference pixel (chosen after lack of reported volcanic unrest in that region based on literature review), and that similar atmospheric conditions exist within two points at a close distance and at similar elevations, which would result in the cancellation of noise caused by atmospheric delay and a smoother time series.

2.4. Volcano deformation modeling

The location, and depth of the best fitting Mogi sources [10] were estimated using an Annealing inversion technique with the GeodMod software developed at the University of Miami. These are flat earth models that assume a pressure source in a homogeneous, isotropic, elastic half-space. The corrected average LOS velocities of a given time period were used as input data, and the quadtree algorithm was used for subsampling [11].

3. RESULTS - INTERPRETATION

Surface deformation was detected at Mayon, Bulusan, Kanlaon, and Taal volcanoes.

3.1. Taal

The 25 km wide Taal Caldera is located on the island of Luzon in the Philippines. The caldera is partially filled with water forming the Taal Lake, and within the lake lies the island that makes the Taal volcano complex which last erupted in 1977. Deformation is observed at various regions within the area (Fig. 2).

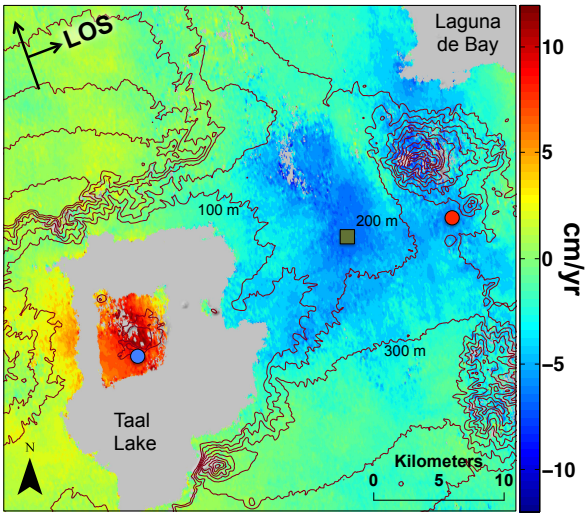

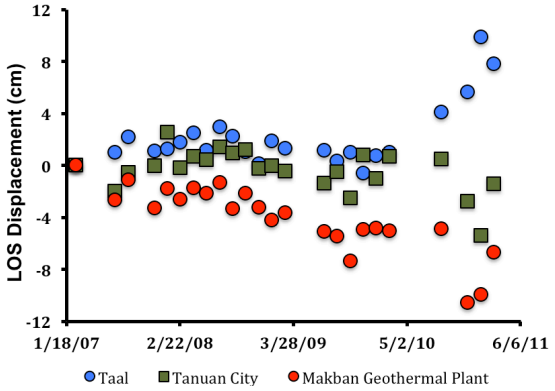

Figure 2. Average LOS velocity for the February 2010 to January 2011 period (top) with reference pixel at 14.446666°N, 120.971389°E; LOS displacement time series (bottom) for the corresponding points shown on the velocity map.

A LOS velocity increase is observed at Taal volcano after February 2010, at a maximum rate of 14.1 cm/yr between February 2010 and January 2011. The signal extends to the western shore of Taal Lake and is likely caused by inflation due to pressurization of the volcanic system. LOS velocity decreases are observed at various regions E-NE of Taal Lake after August 2010. This region makes part of the Macolod Corridor which is a zone characterized by intense volcanism and extensive faulting, with recent volcanism related to NE-SW and NW-SE trending fault systems [12]. The signals are likely related to the faulting systems within the region with the exception of the signal under the Makban Geothermal Plant, which is partly caused by subsidence due to groundwater extraction.

The order of occurrence of the events is remarkable because it could possibly serve as evidence of the magma-tectonic interactions within the region. The results could suggest that pressurization of the magmatic system led to inflation of the volcano, resulting in stress transfers within the region and faulting while the volcano continued to inflate. But further data and modeling is necessary to have an understanding of the interactions occurring within the region, which is out of the scope of this study.

3.2. Mayon

Mayon volcano erupted lava flows during 2006 that were emplaced in the SE flank of the volcano (Smithsonian Institute, Global volcanism report, available at http://www.volcano.si.edu). A LOS velocity decrease is observed at Mayon volcano over these deposits, with a maximum rate of 3.5 cm/yr, likely associated with cooling and compaction (Fig. 3).

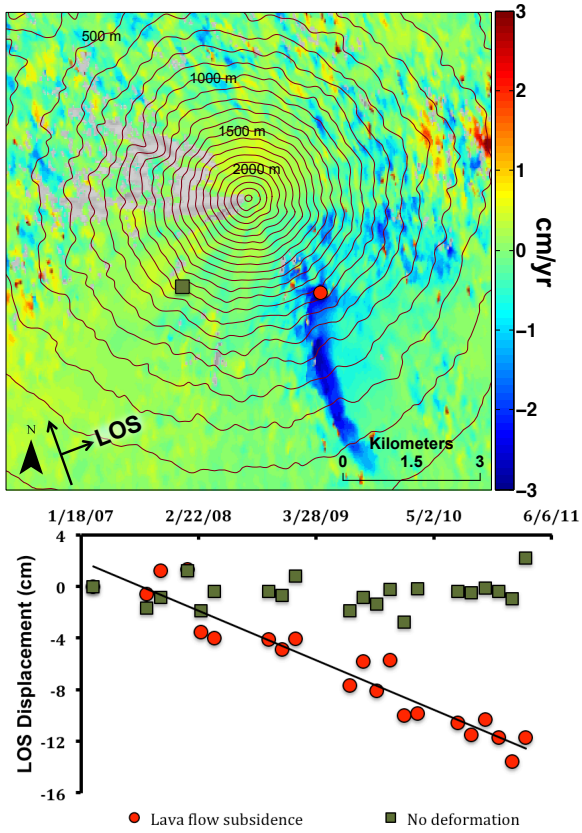

Figure 3. Average LOS velocity for 2007-2011 (top) with reference pixel at 13.406210°N, 123.605000°E; LOS displacement time series (bottom), for the corresponding points shown on the velocity map, with the best fitting linear regression for the deforming point.

3.3. Bulusan

LOS velocity decrease is observed on the Western Flank of Bulusan volcano (Fig. 4), at a maximum rate of 3.5 cm/yr. The signal coincides with the end of the 2007 eruption phase, indicating possible depressurization of the volcanic system.

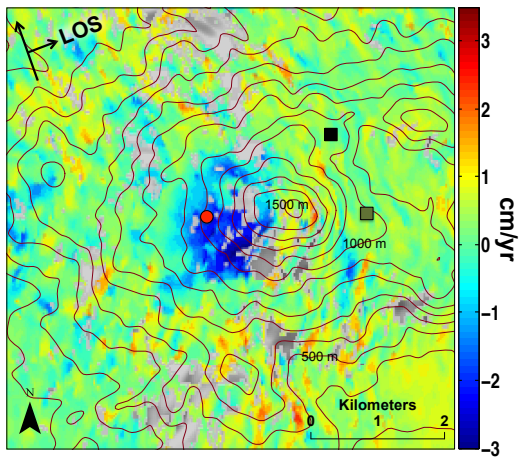

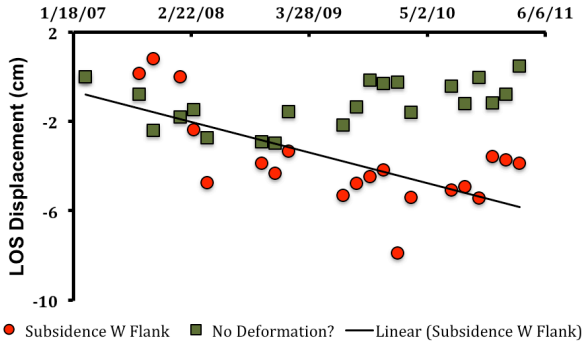

Figure 4. Average LOS velocity for 2007-2011 (top) with reference point shown in black square; LOS displacement time series (bottom), for the corresponding points shown on the velocity map, with the best fitting linear regression for the deforming point.

3.4. Kanlaon

A LOS velocity increase is observed on the Western flank of Kanlaon volcano near the summit (Fig. 5), with a maximum rate of 1.8 cm/yr. The spatial extent of the deforming area is unknown due to the loss of coherence towards the W-SW flank of the volcano. The signal appears to be morphostructurally confined within a valley, and several scarp features can be observed with Google Earth imagery, suggesting that mass movements are the likely cause of the signal.

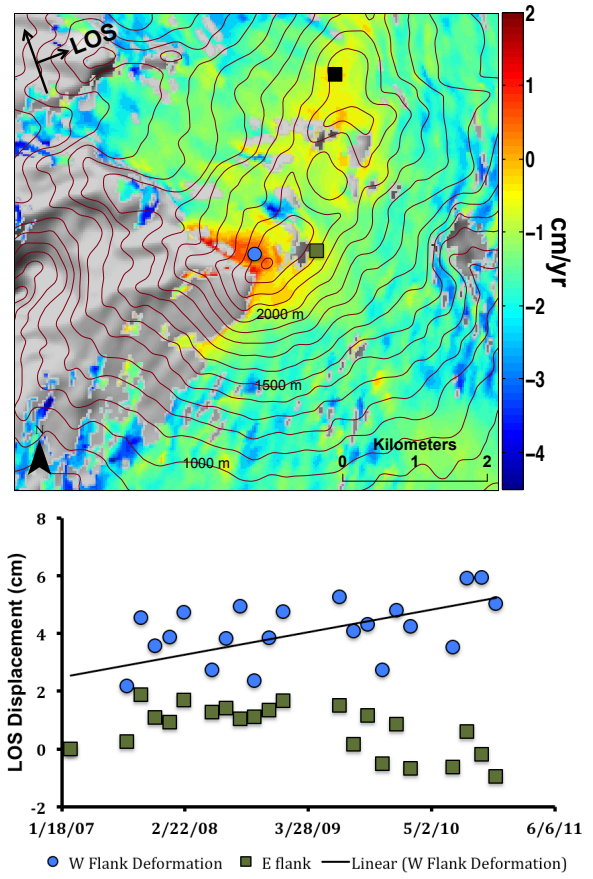

Figure 5. Average LOS velocity for 2007-2011 (top) with reference point shown in black square, and LOS displacement time series (bottom) for the corresponding points shown on the velocity map.

3.5. Volcano deformation modeling

Source models were estimated for Taal and Bulusan volcanoes because the signals detected at these volcanoes are likely related to changes in pressurization of the volcanic systems. The best fitting mogi source model at Taal volcano is centered at 14.0115°N, 121.0024°E (in the NE quadrant of the crater), at a half space depth of 3.07 km with an rms of 17.40 mm (Fig. 6). The best fitting mogi source model at Bulusan volcano is centered at 12.7652°N, 124.0495°E (in the SW flank of the volcano), at a half space depth of 0.50 km with an rms of 5.35 mm (Fig. 7).

Although the point source models are not taking into account the variations in topography, results at Taal would not differ too much considering that it is relatively flat, with the highest elevation at 311m. However, results at Bulusan volcano would most likely vary considering that the summit elevation is at 1565 m. To test this, the source depths were estimated with respect to the summit by assuming that the half space depth is referenced to the average elevation of the subset area. This would give depth estimates with respect to the summit of 3.24 km and 1.47 km for Taal and Bulusan respectively.

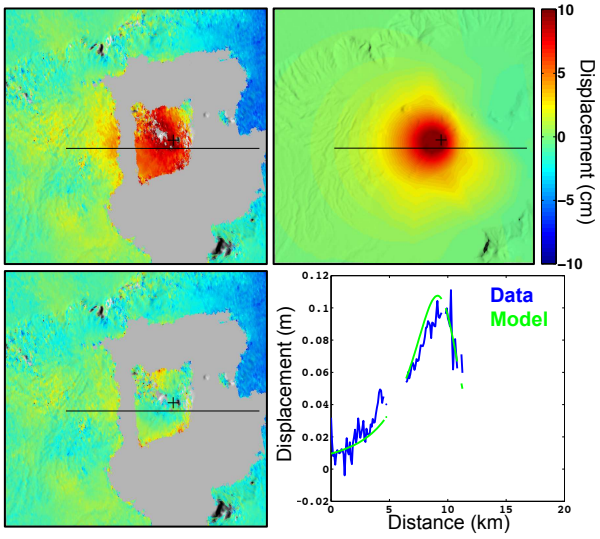

Figure 6. Taal volcano source modeling. Observed data (top left), model prediction (top right), and residual (bottom left), with the location of the Mogi point source displayed as the cross. The black line in all 3 figures represents the extent of the profile (bottom right). The blue profile represents the observed data, and the green profile represents the predicted model.

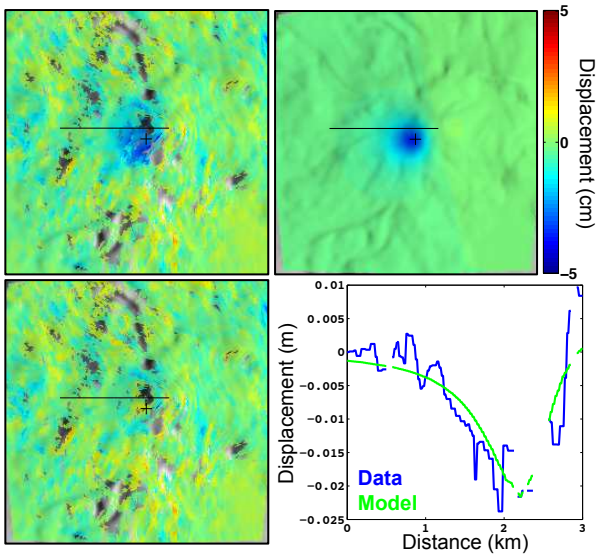

Figure 7. Bulusan volcano source modeling. Observed data (top left), model prediction (top right), and residual (bottom left), with the location of the Mogi point source displayed as the cross. The black line in all 3 figures represents the extent of the profile (bottom right). The blue profile represents the observed data, and the green profile represents the predicted model.

4. DISCUSSION

The results show that deformation was detected at all four targeted volcanoes, relating to changes in pressurization of the volcanic systems only for Taal and Bulusan volcanoes. We further discuss our findings for these two volcanoes.

Two previous studies used GPS data to model the source of inflation at Taal volcano [13; 14]. Reference [13] estimated a source depth of 5.2 km centered at 14.021°N, 120.999°E for the 2000 inflationary period, with a maximum inflation rate of 22 cm/yr. Reference [14] estimated a source depth of 5.1 km centered at 14.013°N, 121.003°E for the 2005 inflationary period, with a maximum inflation rate of 18 cm/yr. Our study used InSAR LOS data to model the inflation source, and our results best agree with the location of the source center estimated by [14], in the NE quadrant of the crater. However, our results place the source center at a shallower depth. This difference can arise due to several factors that need to be addressed in the future. Our models are built using LOS displacement because we only had access to ascending data at the time of the study. Future work should combine ascending with descending data to better constrain the amount of displacement attributed to vertical and horizontal movements. However, the possibility of migration of magma to shallower depths cannot be discarded. Reference [15] suggests intrusion of fresh magma rising to shallower depths during the 2010 volcanic unrest period, as noted by changes in gas emission ratios of CO_2/SO2, CO_2/H_2O and SO_2/H_2S from fumaroles in the Taal Main Crater Lake. A shallow degassing magma connected to a deeper magma chamber beneath the eastern flank of Taal Volcano could also be related to the surface deformation in the eastern section of the volcano [16].

Steaming features were reported by PHIVOLCS on the SW flank after an eruption on October 2007, and edifice deflation during 2009 (Smithsonian Institute, Global volcanism report, available at http://www.volcano.si.edu), but magmatic source characteristics had yet to be constrained. We do not observe edifice deflation in Bulusan, but deflation appears to be localized on the W-SW flank of the volcano which we interpreted to be caused by depressurization of a shallow magmatic source (Fig. 7). The July 2007 eruption at Bulusan volcano produced a 5-km high eruption column and dispersed fallout tephra covering up to 220 km^2 west of the volcano. A lack of juveniles from the tephra based on petrological and X-ray fluorescence analysis suggests that the eruption may have been induced by fragmentation of vent-rocks within the volcano during the phreatic eruption. This implies that there was no fresh magma involved during the eruption [17], and therefore the deformation could also be related to hydrothermal processes.

5. CONCLUSIONS

Following the InSAR time series analysis, we conclude that all of the targeted volcanoes exhibited deformation during the 2007-2011 period. Deformation at Taal and Bulusan volcanoes likely resulted from changes in pressurization of shallow magmatic sources, although other processes could also account for the observed deformation. Source models provided insights into the magma chamber depths and locations. Deformation at Mayon resulted from cooling and compaction of lava flows, while deformation at Kanlaon was attributed to local mass movements.

6. ACKNOWLEDGEMENTS

The ALOS PALSAR data are copyright of the Japan Aerospace Exploration Agency (JAXA) and the Japanese Ministry of Economy, Trade, and Industry (METI). These data were made available through the Alaska Satellite Facility (ASF).

7. REFERENCES

1. Chaussard, E. & Amelung, F. (2012). Precursory inflation of shallow magma reservoirs at west Sunda volcanoes detected by InSAR, *Geophys. Res. Lett.,* **39**(L21311).

2. Chadwick, W.W., Archuleta, R.J. & Swanson, D.A. (1988). The Mechanics of Ground Deformation Precursory to Dome-Building Extrusions at Mount

St. Helens 1981-1982, *J. Geophys. Res.,* **93**(B5), 4351-4366.

3. Werner, C., Wegmüller, U., Strozzi, T., & Wiesmann, A. (2000). Gamma SAR and interferometric procesing software, *Proceedings of the ERS-ENVISAT Symposium, 16-20 October, Gothenburg, Sweden*.

4. Rosen, P. A., Hensley, S., Peltzer, G., & Simons, M. (2004). Updated repeat orbit interferometry package released, *Eos, Transactions American Geophysical Union*, *85*(5), 47-47.

5. Chen, C. W., & Zebker, H. A. (2001). Two-dimensional phase unwrapping with use of statistical models for cost functions in nonlinear optimization, *Journal of the Optical Society of America. A, Optics, image science, and vision*, *18*(2), 338-351.

6. Berardino, P., Fornaro, G., Lanari, R., & Sansosti, E. (2002), A new algorithm for surface deformation monitoring based on small baseline differential SAR interferograms, *IEEE Transactions on Geoscience and Remote Sensing*, *40*(11), 2375-2383.

7. Fattahi, H., & Amelung, F. (2013), DEM Error Correction in InSAR Time Series, *Geoscience and Remote Sensing, IEEE Transactions on*, *51*(7), 4249-4259.

8. Massonnet, D., & Feigl, K.L. (1998), Radar interferometry and its application to changes in the Earth's surface, *Reviews of Geophysics*, *36*(4), 441-500.

9. Chaussard, E., Amelung, F., & Aoki, Y. (2013), Characterization of open and closed volcanic systems in Indonesia and Mexico using InSAR time series, *Journal of Geophysical Research: Solid Earth*, *118*(8), 3957-3969.

10. Mogi, K. (1958), Relations between eruptions of various volcanoes and the deformations of the ground surfaces around them, *Bull. Earthq. Res. Inst.*, 36, 99–134.

11. Jonsson, S., Zebker, H., Segall, P., & Amelung, F. (2002), Fault slip distribution of the 1999 Mw 7.1 Hector Mine, California earthquake, estimated from satellite radar and GPS measurements, *Bull. Seismol. Soc. Am.*, 92, 1377–1389

12. Förster, H., Oles, D., Knittel, U., Defant, M.J., & Torres, R.C. (1990), The Malocod Corridor: A rift crossing the Philippine island arc, *Tectonophysics*, 183.

13. Bartel, B.A., Hamburger, M.W., Meertens, C.M., Lowry, A.R., Corpuz, E., 2003. Dynamics of active magmatic and hydrothermal systems at Taal Volcano, Philippines, from continuous GPS measurements, *J. Geophys. Res.*, 108 (B10).

14. Galgana, G.A., Newman, A.V., Hamburger, M.W., & Solidum, R.U., 2014. Geodetic observations and modeling of time-varying deformation at Taal Volcano, Philippines*, Journal of Volcanology and Geothermal Research*, vol. 271, 1.

15. Arpa, M.C., Hernandez, P.A., Padron, E., Reniva, P., Padilla, G.D., Bariso, E., Melian, G.V., Barrancos, J., Nolasco, D., Calvo, D., Perez, N.M & Solidum, R.U. (2013). Geochemical evidence of magma intrusion inferred from diffuse CO_2 emissions and fumarole plume chemistry: the 2010-2011 volcanic unrest at Taal Volcano, Philippines, *Bull. Volcanol 75*:747.

16. Kumagai, H., Lacson, R., Maeda, Y., Figueroa, M.S., & Yamashina, T. (2014). Shallow S wave attenuation and actively degassing magma beneath Taal Volcano, Philippines, *Geophysical Research Letters*, 41, 6681-6888.

17. Delos Reyes, P., Bornas, M.A., Arpa, M.C., Laguerta, E., Cahulogan, M., Maximo, R.P., Mirabueno, M.H., Perez, J., Tubianosa, B., Solidum, R. (2014). Fallout Tephras of the 2006-2007 Eruptions of the Bulusan Volcano, Southern Luzon, Philippines, *Journal of Geography*, 123(5), 761-775.